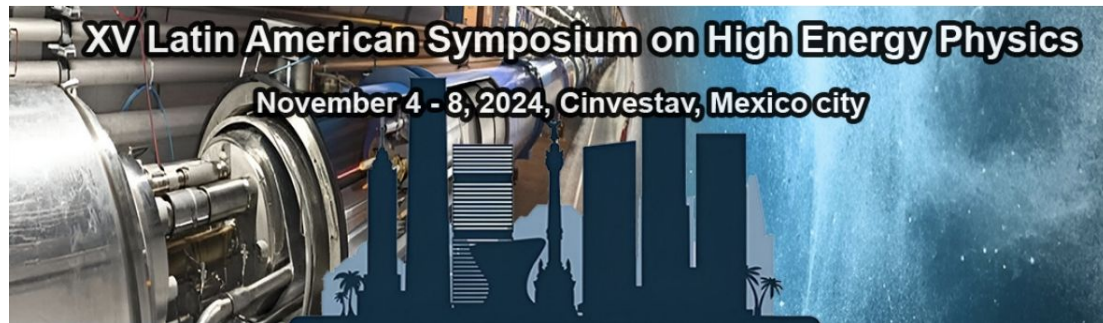
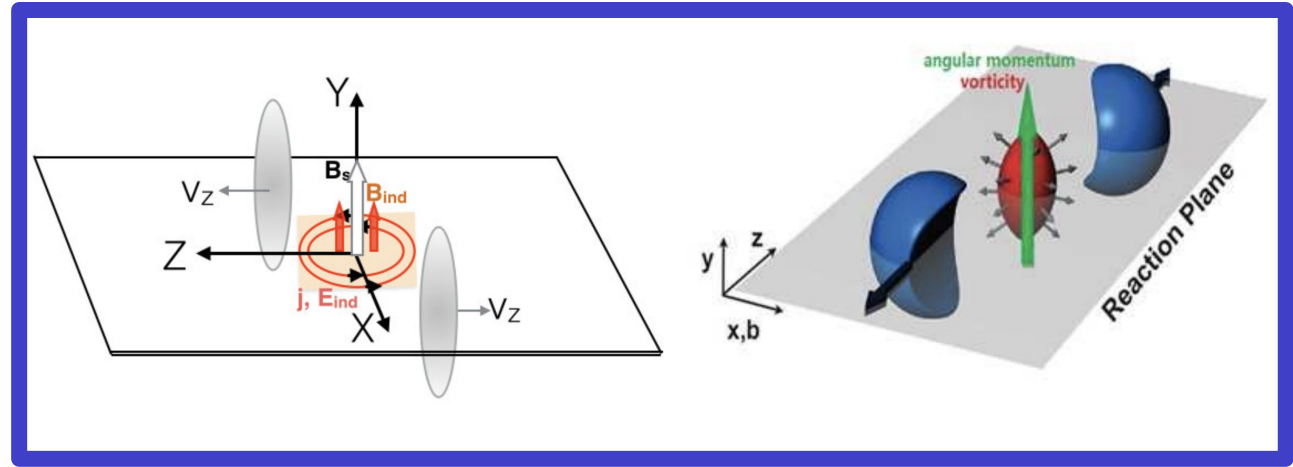


Exploring Multiple QCD Phase Diagrams

Luis Alberto Hernández Rosas
Universidad Autónoma Metropolitana



CONTENT

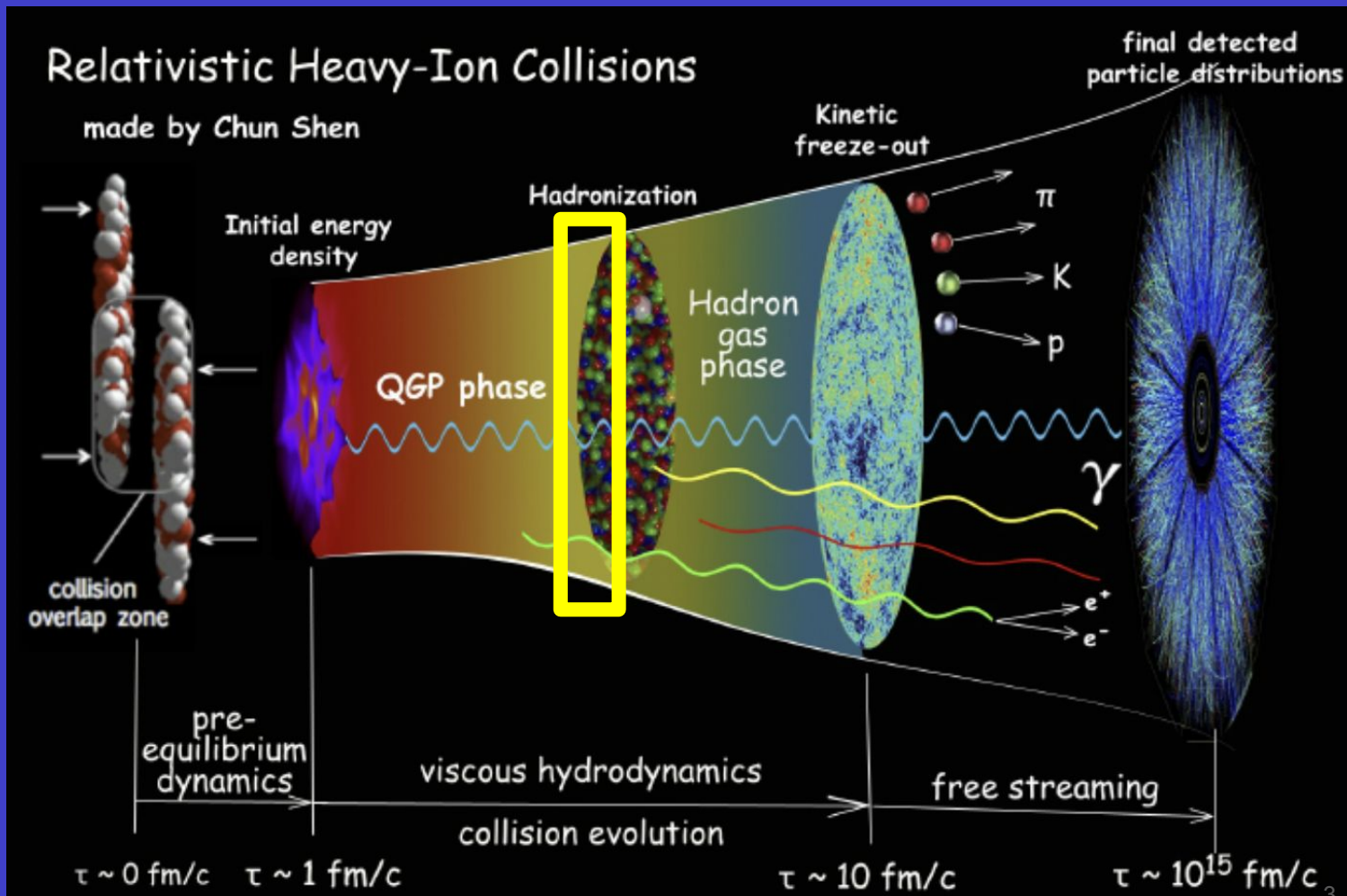


- PHYSICS MOTIVATION

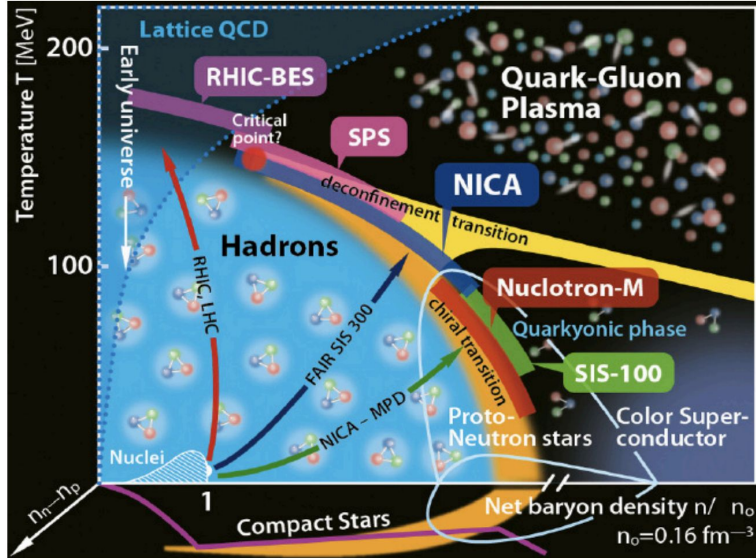
- LSMq AND THE EFFECTIVE POTENTIAL

- PHASE DIAGRAMS & FINAL REMARKS

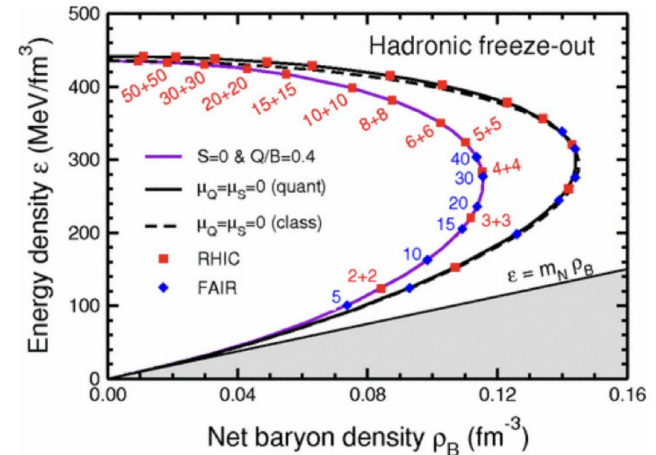
HIC



QCD Phase Diagram \leftrightarrow Heavy-ion Collisions



Different T and μ_B combinations
 \rightarrow Different collision energies in HIC



QCD PHASE TRANSITION IS A NON PERTURBATIVE PHENOMENON

Linear Sigma model coupled to quarks

Effective theory which is useful to emulate the low energy regime of Quantum Chromodynamics. It exhibits a symmetry spontaneously broken.

$$\mathcal{L} = \frac{1}{2}(\partial_\mu\sigma)^2 + \frac{1}{2}(\partial_\mu\vec{\pi})^2 + \frac{a^2}{2}(\sigma^2 + \vec{\pi}^2) - \frac{\lambda}{4}(\sigma^2 + \vec{\pi}^2)^2 + i\bar{\psi}\gamma^\mu\partial_\mu\psi - ig\bar{\psi}\gamma^5\vec{\tau}\cdot\vec{\pi}\psi - g\bar{\psi}\psi\sigma$$

letting the sigma-field to develop a vacuum expectation value v , we have

$$V^{tree} = -\frac{a^2}{2}v^2 + \frac{\lambda}{4}v^4$$

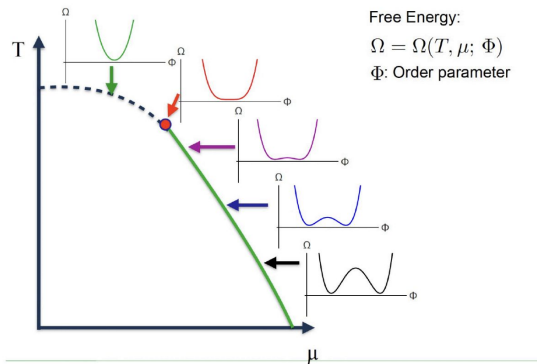
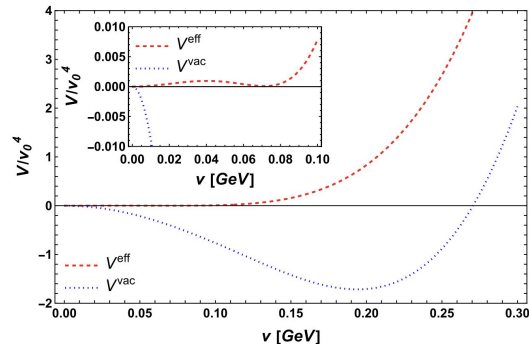
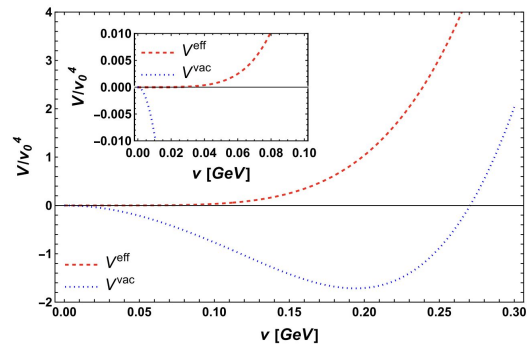

$$\sigma \rightarrow \sigma + v$$

$$a^2, \lambda, g$$

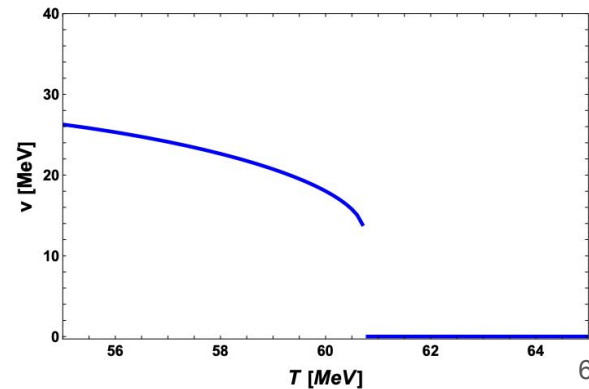
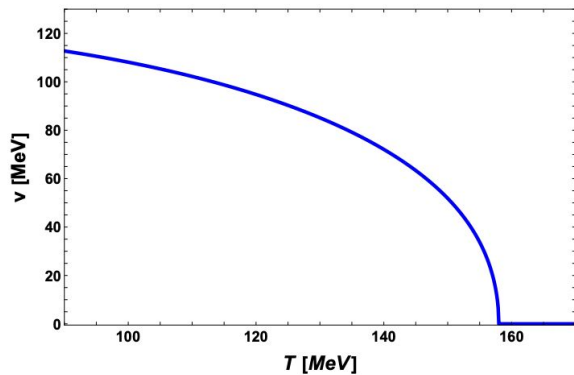
$$m_\sigma^2 = 3\lambda v^2 - a^2, \quad m_0^2 = \lambda v^2 - a^2, \quad m_f = gv$$

CHIRAL SYMMETRY RESTORATION

v = vacuum expectation value \rightarrow order parameter



low $\leftarrow \mu_q \rightarrow$ high



EFFECTIVE POTENTIAL

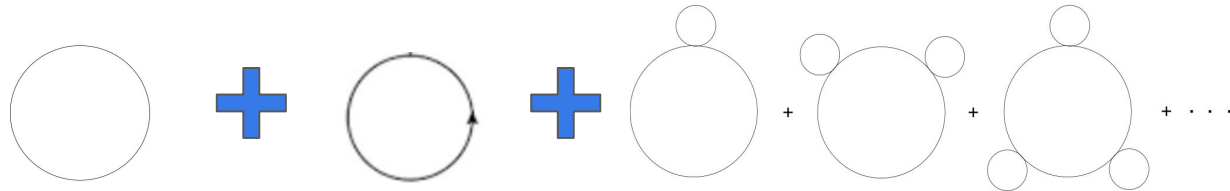
**Imaginary Time
Formalism**

$$V^{\text{eff}} = V^{\text{tree}} + V_b^1 + V_f^1 + V^{\text{rings}}$$

$$V_b^1 = -\frac{i}{2} \int \frac{d^4 k}{(2\pi)^4} \ln(D_b^{-1}(k)) \quad , \quad V_f^1 = iN_c \int \frac{d^4 k}{(2\pi)^4} \text{Tr}[\ln(S_f^{-1}(k))]$$

screening effects

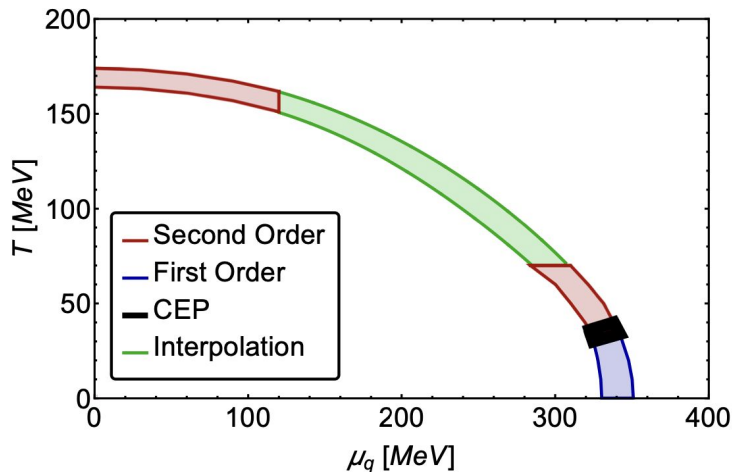
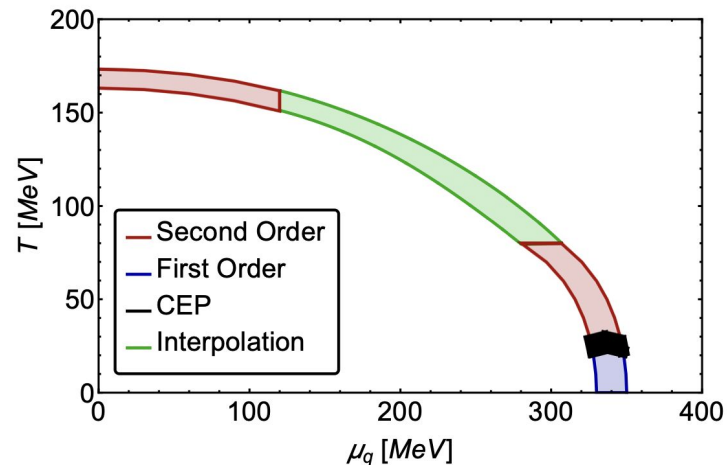
$$V^{\text{ring}} = \frac{T}{2} \sum_{n=-\infty}^{\infty} \int \frac{d^3 k}{(2\pi)^3} \ln(1 + \Pi D(\omega_n, \Omega, \vec{k})),$$



WE GO BACK TO 2018

- Effective potential with the LSMq at finite T and μ_q in the high- and low- T approximation.
- 2nd order and 1st order phase transition.
- CEP appears.

A. Ayala, S. Hernandez-Ortiz and LAH, Rev. Mex. Fis. **64**, no.3, 302-313 (2018)

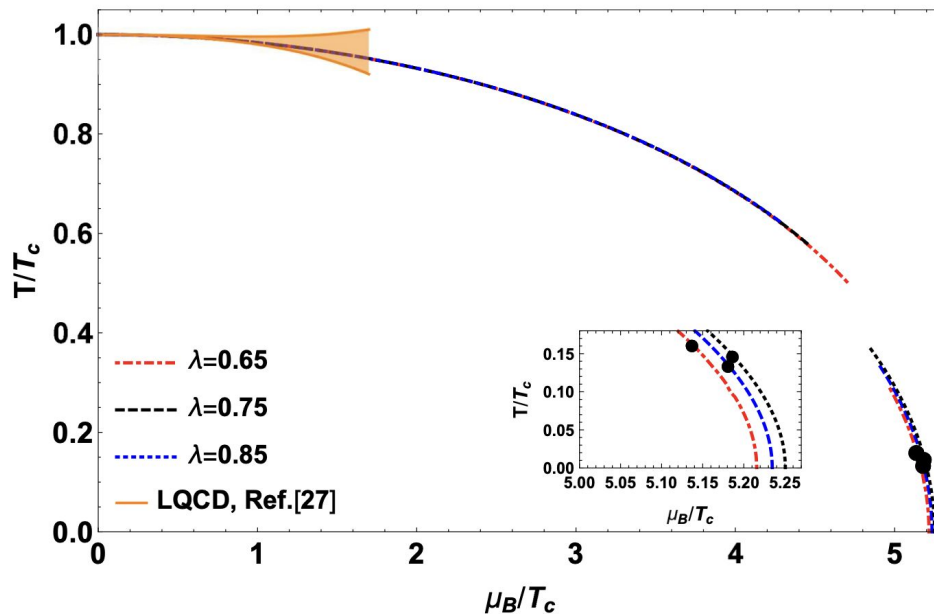


Two different sets of λ , g and a

IMPROVING RESULTS

- Effective potential with the LSMq at finite T and μ_q in the high- and low-T approximation.
- 2nd order and 1st order phase transition.
- CEP appears.
- **Following LQCD curvature**

A. Ayala, [LAH](#), M. Loewe, J. C. Rojas and R. Zamora, *Eur. Phys. J. A* **56**, no.2, 71 (2020)

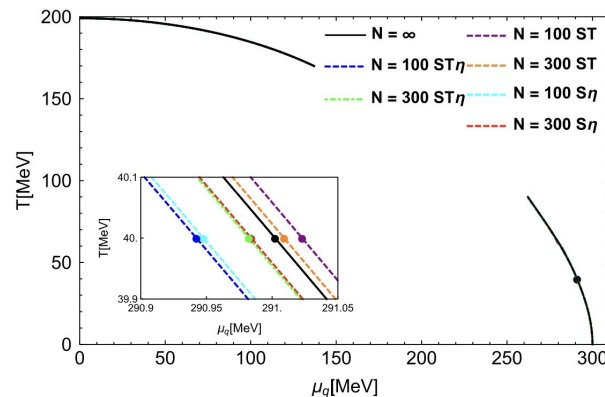
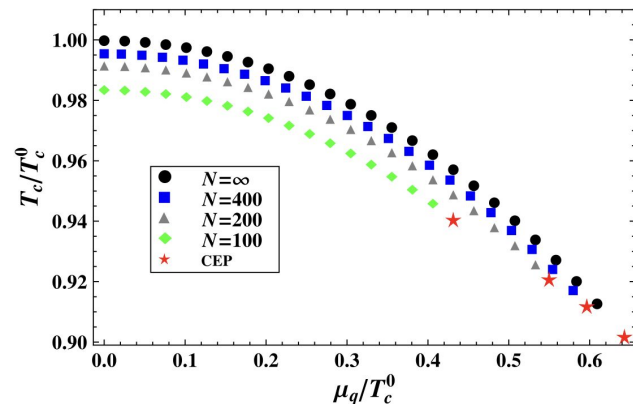


NEW INGREDIENTS

- Effective potential with the LSMq at finite T and μ_q in the high- and low-T approximation.
- 2nd order and 1st order phase transition.
- CEP appears.
- Following LQCD curvature
- **Superstatistics**

A. Ayala, M. Hentschinski, [LAH](#), M. Loewe and R. Zamora, Phys. Rev. D **98**, no.11, 114002 (2018)

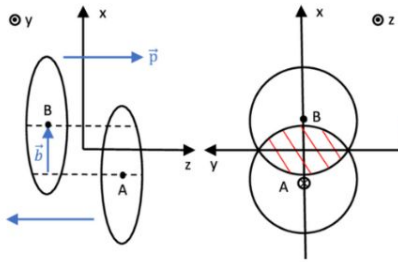
A. Ayala, S. Hernandez-Ortiz, [LAH](#), V. Knapp-Perez and R. Zamora, Phys. Rev. D **101**, no.7, 074023 (2020)



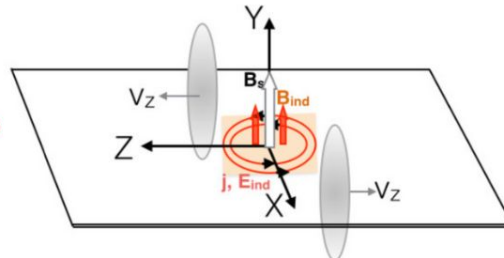
HICs

1. **Phase transition**
Quark-Gluon Plasma → Chiral Symmetry
2. **Baryon Chemical Potential**
Region of maximum baryon density (MPD-NICA)
3. **Effective models**
Low energies of QCD
4. **Non-central collisions**
Finite Impact Parameter \mathbf{b}
5. **Angular velocity**
Maximum value $\sim 0.1 \text{ fm}^{-1}$ ($\sim 20 \text{ MeV}$)
6. **Magnetic Fields**
Short pulse with maximum high $\sim (m_{\pi})^2$
7. **Collision Energy**
Effects more important at low energies

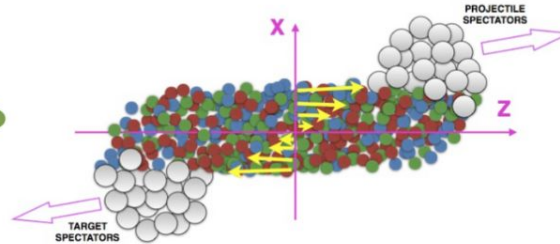
NON CENTRAL COLLISION



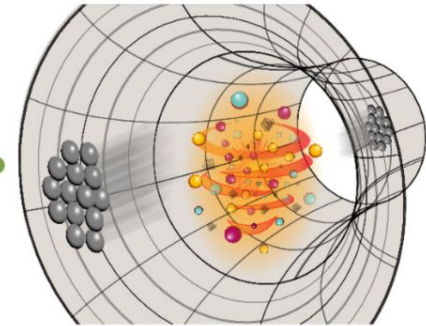
Eur.Phys.J.C 83 (2023) 1, 96



Phys.Rev.C 96 (2017) 5, 054909

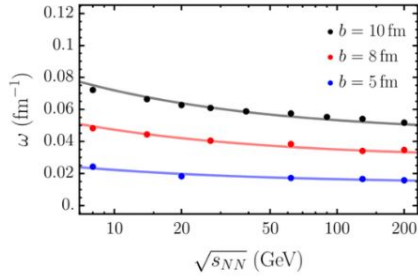


EPJ Web Conf. 171 (2018) 07002

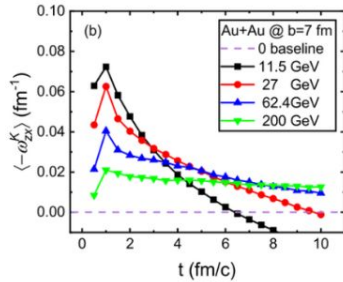


Nucl.Sci.Tech. 34 (2023) 1, 15

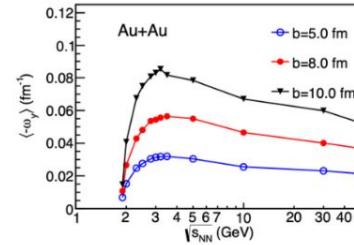
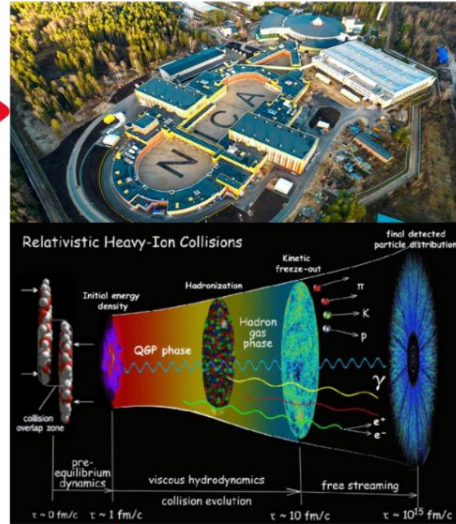
ANGULAR VELOCITY



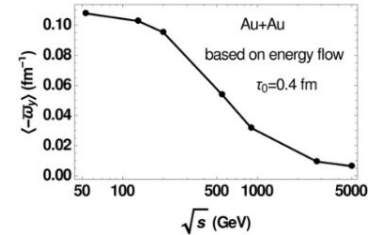
Initial angular velocity ω for Au + Au collisions at impact parameters $b = 5, 8, 10$ fm as functions of collision energy (UrQMD). Phys. Rev. D **102** (2020), 056019



Time evolution of angular velocity at $b = 7$ fm and four different energies (PACIAE). Phys. Rev. C **104** (2021) 5, 054903

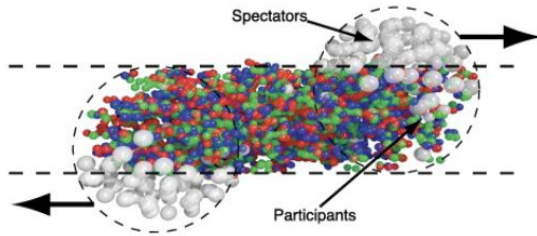


Initial angular velocity at mid rapidity as a function of the collision energy for impact parameters $b = 5, 8$, and 10 fm (UrQMD). Phys. Rev. C **101** (2020) 6, 064908

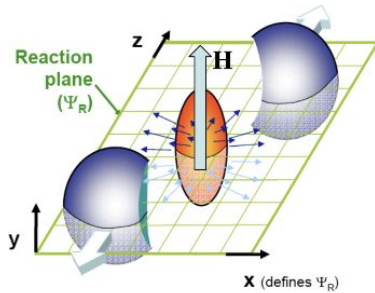


Angular velocity at fixed $\tau = 0.4$ fm and $\eta = 0$ as function of collision energy (HIJING). Phys. Rev. C **93** (2016), 064907

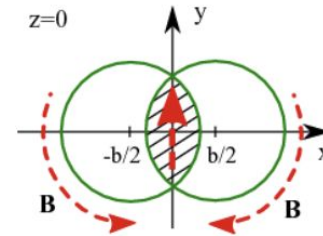
MAGNETIC FIELDS



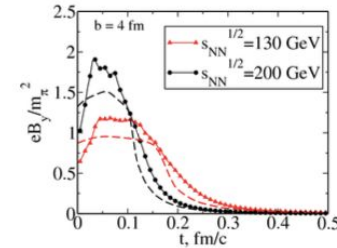
R. Snellings, J. Phys. **13**, (2011) 055008



D. E. Kharzeev, L. D. McLerran and H. J. Warringa, Nucl. Phys. A **803**, 227 (2008)

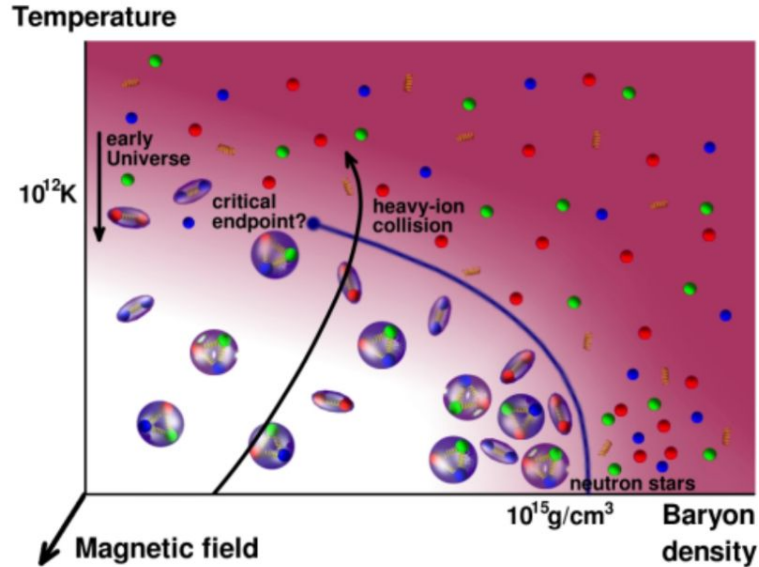


V. Voronyuk *et al.*, Phys. Rev. C **83**, 054911 (2011)

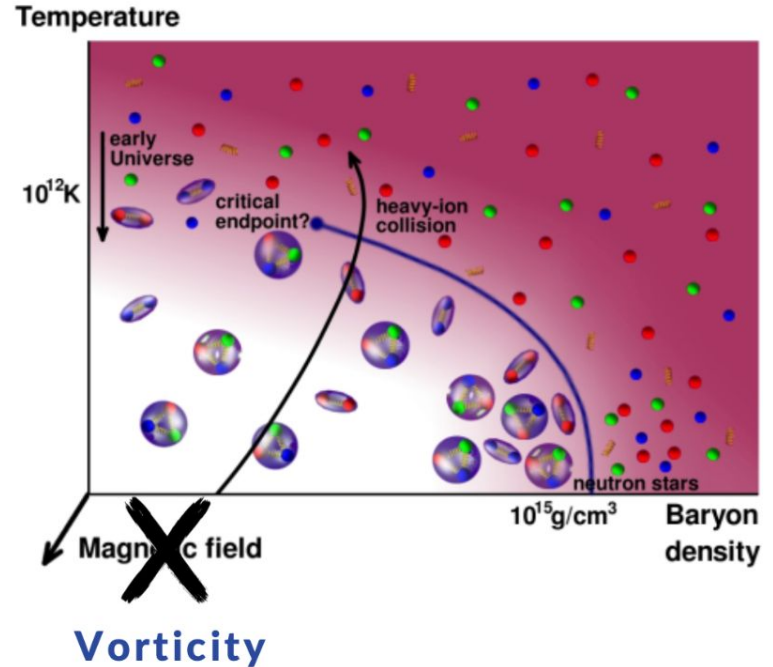


V. Skokov, A. Y. Illarionov and V. Toneev, Int. J. Mod. Phys. A **24**, 5925 (2009)

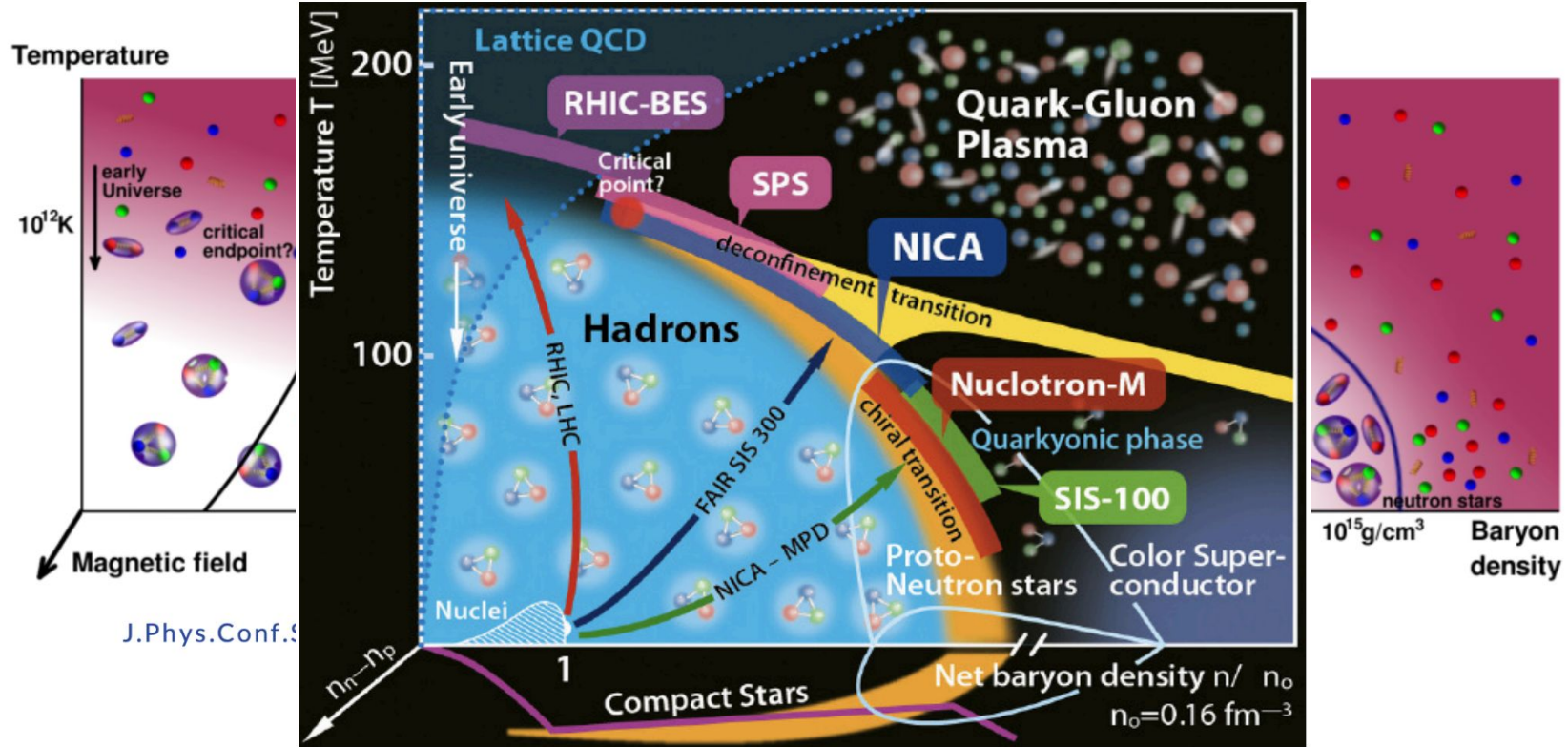
QCD phase diagram



J.Phys.Conf.Ser. 503 (2014) 012009



QCD phase diagram



Linear Sigma model coupled to quarks

Effective theory which is useful to emulate the low energy regime of Quantum Chromodynamics. It exhibits a symmetry spontaneously broken.

$$\mathcal{L} = \frac{1}{2}(\partial_\mu\sigma)^2 + \frac{1}{2}(\partial_\mu\vec{\pi})^2 + \frac{a^2}{2}(\sigma^2 + \vec{\pi}^2) - \frac{\lambda}{4}(\sigma^2 + \vec{\pi}^2)^2 + i\bar{\psi}\gamma^\mu\partial_\mu\psi - ig\bar{\psi}\gamma^5\vec{\tau}\cdot\vec{\pi}\psi - g\bar{\psi}\psi\sigma$$

letting the sigma-field to develop a vacuum expectation value v , we have

$$V^{tree} = -\frac{a^2}{2}v^2 + \frac{\lambda}{4}v^4$$


$$\sigma \rightarrow \sigma + v$$

$$a^2, \lambda, g$$

$$m_\sigma^2 = 3\lambda v^2 - a^2, \quad m_0^2 = \lambda v^2 - a^2, \quad m_f = gv$$

EFFECTIVE POTENTIAL

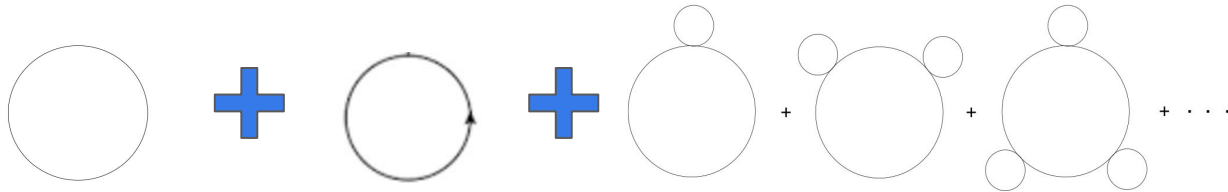
**Imaginary Time
Formalism**

$$V^{\text{eff}} = V^{\text{tree}} + V_b^1 + V_f^1 + V^{\text{rings}}$$

$$V_b^1 = -\frac{i}{2} \int \frac{d^4 k}{(2\pi)^4} \ln(D_b^{-1}(k)) \quad , \quad V_f^1 = iN_c \int \frac{d^4 k}{(2\pi)^4} \text{Tr}[\ln(S_f^{-1}(k))]$$

screening effects

$$V^{\text{ring}} = \frac{T}{2} \sum_{n=-\infty}^{\infty} \int \frac{d^3 k}{(2\pi)^3} \ln(1 + \Pi D(\omega_n, \Omega, \vec{k})),$$



PROPAGATORS

Finite eB

Boson

$$D(p) = \int_0^\infty \frac{ds}{\cos(|q_b B|s)} e^{is \left(p_\parallel^2 - p_\perp^2 \frac{\tan(|q_b B|s)}{|q_b B|s} - m_b^2 + i\epsilon \right)},$$

Fermion

$$\begin{aligned} S_f(p) &= \int_0^\infty \frac{ds}{\cos(|q_f B|s)} e^{is \left(p_\parallel^2 - p_\perp^2 \frac{\tan(|q_f B|s)}{|q_f B|s} - m_f^2 + i\epsilon \right)} \\ &\times \left[\left(\cos(|q_f B|s) + \gamma_1 \gamma_2 \sin(|q_f B|s) \text{sign}(q_f B) \right) \right. \\ &\times \left. \left(m_f + \not{p}_\parallel \right) - \frac{\not{p}_\perp}{\cos(|q_f B|s)} \right], \end{aligned}$$

Phys.Rev. 82 (1951) 664-679

Finite Ω

Boson

$$D(p) = \frac{1}{(p_0 + \Omega)^2 - p_\perp^2 - p_z^2 - m^2 + i\epsilon}$$

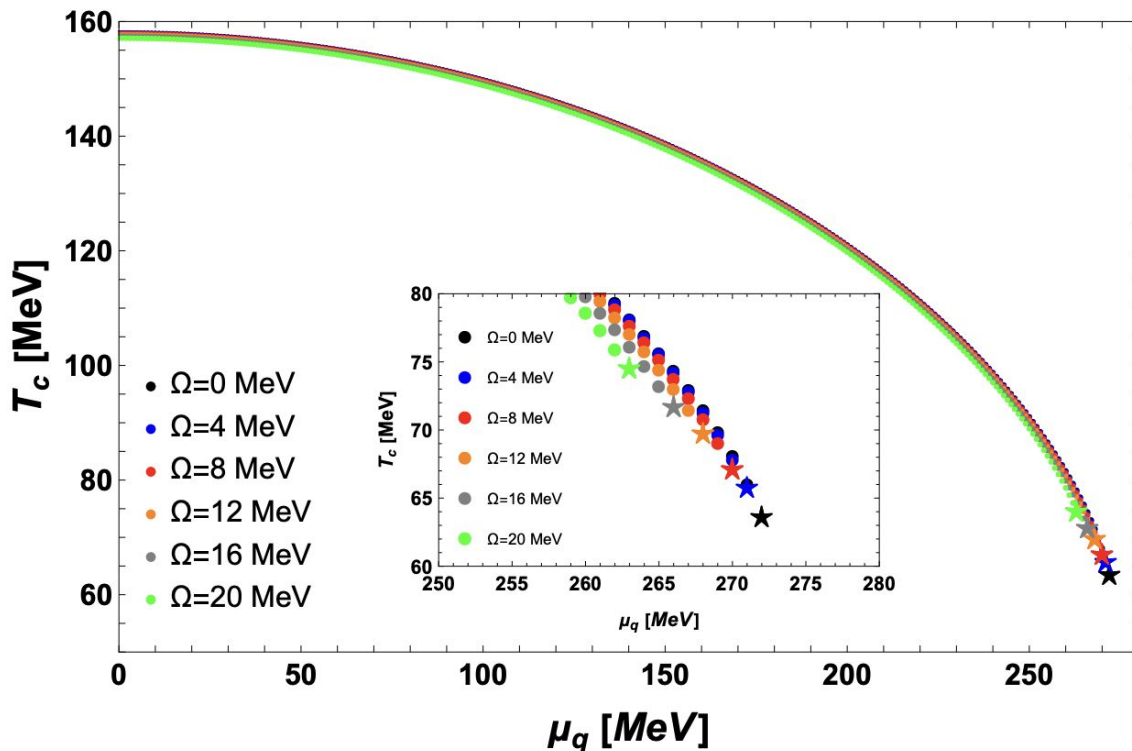
Phys.Rev.D 108 (2023) 9, 094020

Fermion

$$\begin{aligned} S(p) &= \frac{(p_0 + \Omega/2 - p_z + ip_\perp)(\gamma_0 + \gamma_3) + m(1 + \gamma_5)}{(p_0 + \Omega/2)^2 - \vec{p}^2 - m^2 + i\epsilon} \mathcal{O}^+ \\ &+ \frac{(p_0 - \Omega/2 + p_z - ip_\perp)(\gamma_0 - \gamma_3) + m(1 + \gamma_5)}{(p_0 - \Omega/2)^2 - \vec{p}^2 - m^2 + i\epsilon} \mathcal{O}^-, \end{aligned}$$

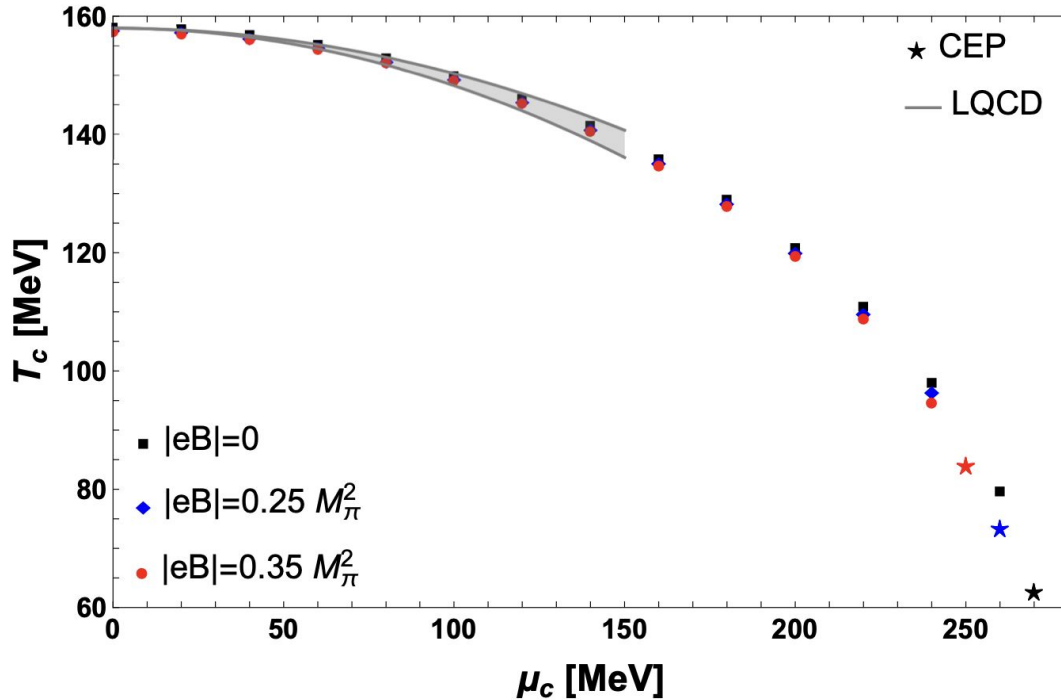
Phys.Rev.D 103 (2021) 7, 076021

PHASE DIAGRAM Ω



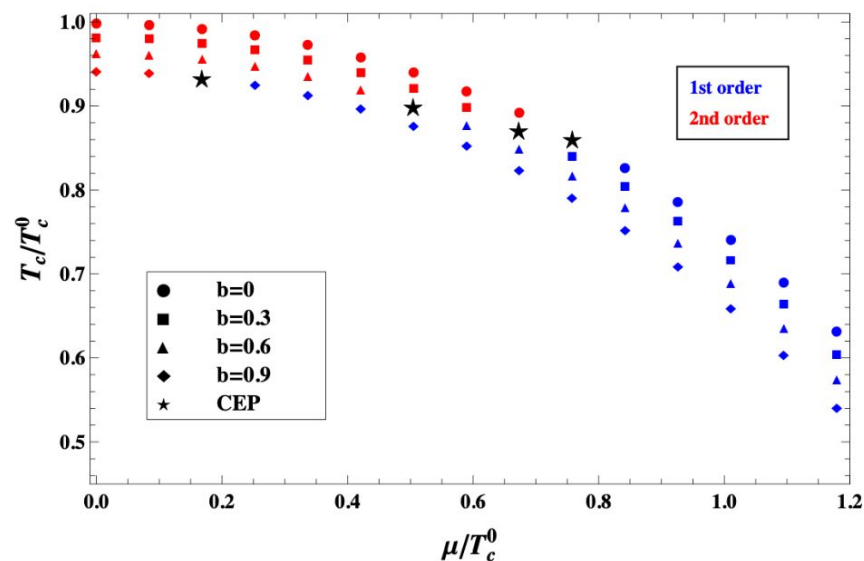
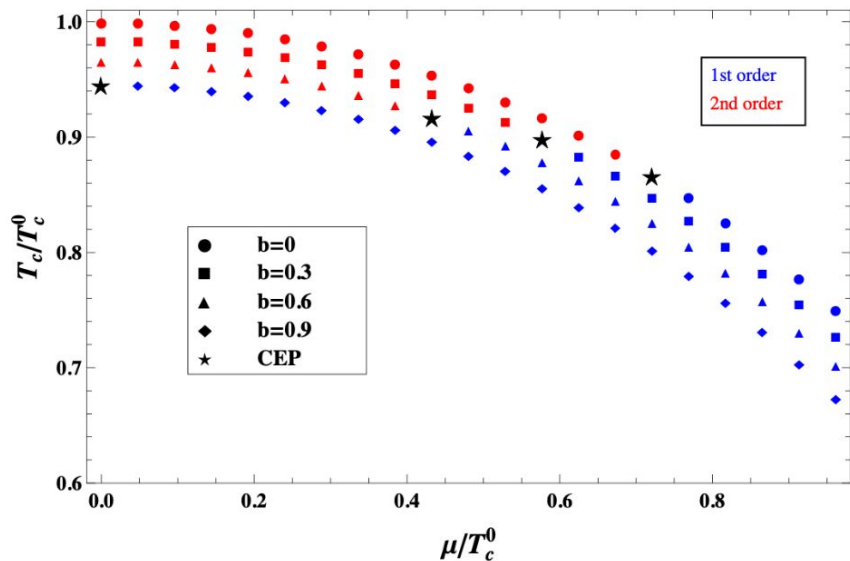
- The T_c decreases as the Ω increases.
- Larger Ω moves the CEP to lower μ_q and higher T .
- The Ω not only modifies the conditions under which the phase transition occurs, but also the nature of the transition

PHASE DIAGRAM eB



- The T_c decreases as the eB increases.
- Larger eB moves the CEP to lower μ_q and higher T .
- The eB not only modifies the conditions under which the phase transition occurs, but also the nature of the transition

THE TRUE BEGINNING



Inverse Magnetic Catalysis was obtained

SUMMARY

- The LSMq has been successful in exploring the phase transition of QCD.
- The possible location of the CEP has been inspected
- **T- μ_B plane + eB , Ω , eE , μ_I or ...**
- Translating phase diagram information into observables in HIC

**Thanks for
your
attention!**

`lhernandez.rosas@izt.uam.mx`
`luis.hr@xanum.uam.mx`

BARYON NUMBER FLUCTUATION

Conserved Charges: Net Baryon Number (B), Net Charge (Q), Net Strangeness (S)

Measured multiplicity N , $\langle \delta N \rangle = N - \langle N \rangle$

mean: $M = \langle N \rangle = C_1$

variance: $\sigma^2 = \langle (\delta N)^2 \rangle = C_2$

skewness: $S = \langle (\delta N)^3 \rangle / \sigma^3 = C_3 / C_2^{3/2}$

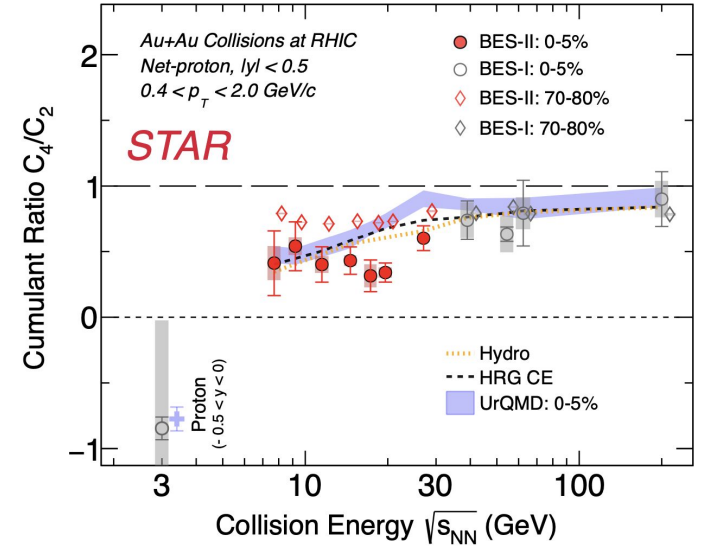
kurtosis: $\kappa = \langle (\delta N)^4 \rangle / \sigma^4 - 3 = C_4 / C_2^2$

Moments, cumulants and susceptibilities:

2nd order: $\sigma^2 / M \equiv C_2 / C_1 = \chi_2 / \chi_1$

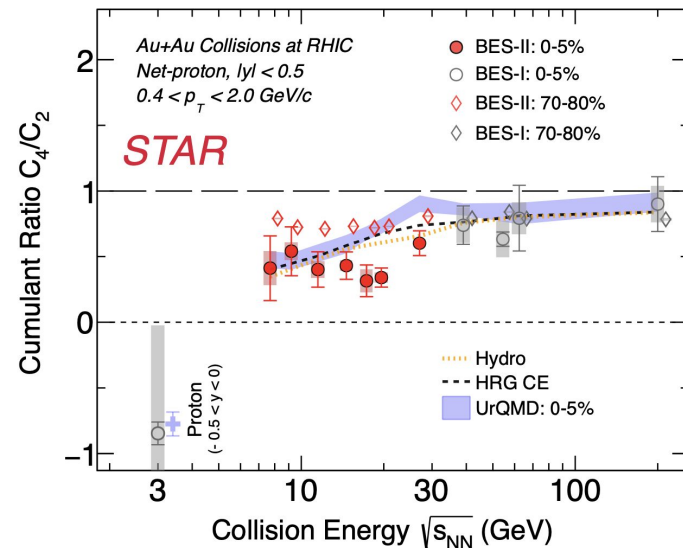
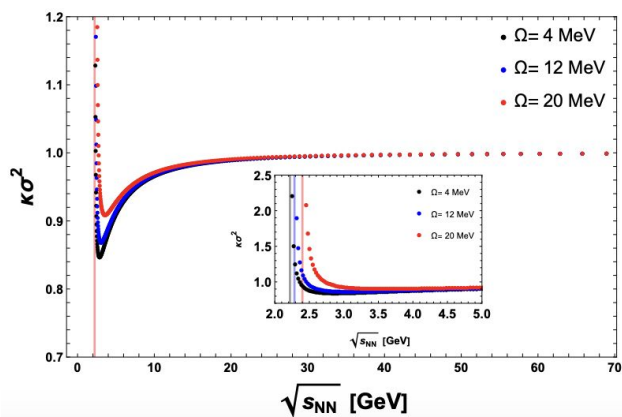
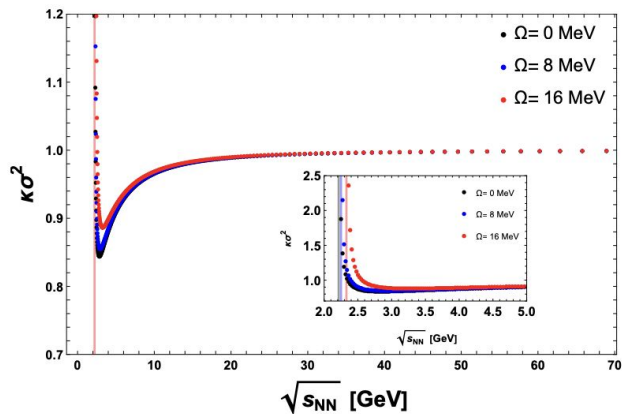
3rd order: $S \sigma \equiv C_3 / C_2 = \chi_3 / \chi_2$

4th order: $\kappa \sigma^2 \equiv C_4 / C_2 = \chi_4 / \chi_2$



A. Pandav (STAR collaboration), plenary talk at CPOD 2024,
<https://conferences.lbl.gov/event/1376/contributions/8772/>

BARYON NUMBER FLUCTUATION



A. Pandav (STAR collaboration), plenary talk at CPOD 2024, <https://conferences.lbl.gov/event/1376/contributions/8772/>

SUMMARY 2.0

- As the energy approaches the CEP position, the fourth moment exhibits a sharp increase, suggesting that the CEP location can be identified by this abrupt rise. This behavior is also influenced by vorticity, as higher values of Ω shift the CEP to higher collision energies.